Mol Biotechnol (2016) 58:540–550
DOI 10.1007/s12033-016-9951-0

ORIGINAL PAPER

Development of a Low-Cost Stem-Loop Real-Time Quantification PCR Technique for EBV miRNA Expression Analysis

Massimiliano Bergallo[1,2] · Chiara Merlino[1] · Davide Montin[3] · Ilaria Galliano[1,2] · Stefano Gambarino[2] · Katia Mareschi[4] · Franca Fagioli[4] · Paola Montanari[1,3] · Silvana Martino[1,4] · Pier-Angelo Tovo[1,2,3]

Published online: 31 May 2016

Abstract MicroRNAs (miRNAs) are short, single stranded, non-coding RNA molecules. They are produced by many different species and are key regulators of several physiological processes. miRNAs are also encoded by the genomes of multiple virus families, such as herpesvirus family. In particular, miRNAs from Epstein Barr virus were found at high concentrations in different associated pathologies, such as Burkitt's lymphoma, Hodgkin disease, and nasopharyngeal carcinoma. Thanks to their stability, these molecules could possibly serve as biomarkers for EBV-associated diseases. In this study, a stem-loop real-time PCR for miR-BART2-5p, miR-BART15, and miR-BART22 EBV miRNAs detection and quantification has been developed. Evaluation of these miRNAs in 31 serum samples (12 from patients affected by primary immunodeficiency, 9 from X-linked agammaglobulinemia and 10 from healthy subjects) has been carried out. The amplification performance showed a wide dynamic range (10^8–10^2 copies/reaction) and sensibility equal to 10^2 copies/reaction for all the target tested. Serum samples analysis, on the other hand, showed a statistical significant higher level of miR-BART22 in primary immunodeficiency patients ($P = 0.0001$) compared to other groups and targets. The results confirmed the potential use of this assay as a tool for monitoring EBV-associated disease and for miRNAs expression profile analysis.

Keywords miRNA · EBV · Stem-loop real-time PCR · MGB · EBV-associated pathologies

✉ Massimiliano Bergallo
massimiliano.bergallo@unito.it

[1] Department of Public Health and Pediatric Sciences, Medical School, University of Turin, Turin, Italy

[2] Laboratory of Cytoimmunodiagnostics, University Hospital City of Science and Health of Turin, Regina Margherita Children's Hospital, Turin, Italy

[3] S.S. Immunorheumatology, S.C. Pediatria 2, University Hospital City of Science and Health of Turin, Regina Margherita Children's Hospital, Turin, Italy

[4] Pediatric Onco-Hematology, Stem Cell Transplantation and Cellular Therapy Division, City of Science and Health of Turin, Regina Margherita Children's Hospital, Turin, Italy

Introduction

Small regulatory RNAs are short, 20-30-nucleotide-long, single stranded, non-coding RNA molecules with various biological functions. Since the discovery in 1993 of the first small regulatory RNA, lin-4, in *Caenorhabditis elegans*, several classes of small regulatory RNA have been identified in various species. These molecules can be grouped in classes including endogenous and exogenous small interfering RNAs (siRNAs), microRNAs (miRNAs), and Piwi-interacting RNAs (piRNAs) [1]. miRNAs are key regulators of several physiological processes in a wide range of species and experimental systems including embryonic development, cell differentiation, and regulation of immune homeostasis [2, 3]. Furthermore, these molecules play critical roles in different human diseases, including cancers, neurodegenerative disorders, and autoimmune diseases [4–6]. miRNAs are also encoded by the genomes of multiple virus families, such as herpesvirus family that have recently received much attention [7]. With the notable exception of varicella zoster virus, all investigated herpesviruses carry miRNAs in their genomes [7, 8]. Other examples of virus families that encode miRNAs include Polyomaviruses, Baculoviruses, Ascoviruses, Iridoviruses, and Adenoviruses [7]. It is interesting to note

that these virus families share a DNA genome, a nuclear life cycle and, in particular for herpesviruses, the ability to induce latency in infected cells. This raises the question whether RNA viruses cannot encode miRNAs because they have no access to the processing enzymes in the nucleus or because the processing of their miRNAs could have a negative impact on their fitness or their ability to produce high titer progenies. If RNA viruses want to express a miRNA, they have to evolve a strategy to avoid cleavage of the viral RNA genome by the RNAi machinery [9]. Retroviruses have developed unique strategies to evade such problems. The retroviruses bovine leukemia virus and bovine foamy virus use an intragenomic RNAP III promoter to produce subgenomic RNA transcripts that are processed into mature miRNAs in a microprocessor-independent manner [9]. Herpes simplex virus 1 miRNAs prevent entry into lytic viral replication [10] and a similar role has been proposed for the K12 miRNA cluster encoded by Kaposi's sarcoma-associated herpesvirus [11, 12]. EBV microRNAs were discovered by sequencing libraries of small RNAs generated from several EBV-positive cell lines, including BL41/B95-8 Burkitt's lymphoma (BL) cell line, primary effusion lymphoma cell line (PEL-1), EBV-positive BLs, and nasopharyngeal carcinomas (NPC) [13]. EBV encodes multiple miRNAs that target viral and cellular genes [13], with the majority of the miRNAs encoded within 2 primary transcripts, designated BamHI fragment H rightward open reading frame 1 (BHRF1) and BamHI-A region rightward transcript (BART). BHRF1-derived miRNAs were reported to be highly expressed in EBV-positive lymphoblastoid cell lines (LCLs), whereas BART miRNAs have been found in all EBV-infected cell lines, such as LCL, BL, Hodgkin disease, and NPC [13]. Because miRNAs possess high stability and are easily quantified, these molecules could possibly serve as biomarkers for EBV-associated diseases [14–16]. Circulating miRNAs have been identified in the serum and plasma of patients with cancer, and the expression profiles of these miRNAs could have high potential as novel biomarkers in diagnosing human diseases [17, 18]. However, the potential of EBV miRNAs as biomarkers in EBV-associated diseases has not yet been fully explored.

In particular, it could be interesting to study primary immunodeficiencies (PIDs), in which EBV-associated complications are reported, and X-linked agammaglobulinemia (XLA) immunodeficiencies, characterized by the lack of immunoglobulin, B cells, and plasma cells, secondary to mutation in the Bruton's tyrosine kinase (Btk) gene, to evaluate the role of EBV miRNAs in these pathological conditions.

Recently, research on miRNAs has increased sharply due to the growing awareness of their importance. Several methods have been employed to detect the expression of miRNAs in a variety of biological samples, but less abundant miRNAs often escape detection by technologies such as cloning, Northern blot analysis [19] and microarray [20]. Chen et al. [21] proposed a novel real-time quantification method based on the use of a stem loop primer (SLP) for the reliable and sensitive detection of mature miRNAs. This stem-loop real-time quantitative PCR (RT-qPCR) assay (TaqManH small RNA assays) showed a high degree of sensitivity and a broad dynamic range in detecting the expression of miRNAs.

Integration and optimization with Minor groove binders (MGB) technology of this approach were developed in this study, obtaining a cost-effective, highly sensitive and accurate RT-qPCR method for the quantification of mature EBV miR-BART2-5p, miR-BART15, and miR-BART22 molecules. The MGB probe technology utilizes a minor groove binder attached to single-stranded DNA probes to boost the stability and raise the melting temperature (Tm) of the DNA duplex formed when probes bind to complementary targets. The MGB moiety is stabilized in the minor groove by hydrophobic interactions. By attaching the MGB moiety to the 5′-end of a DNA probe during synthesis on a commercial synthesizer the MGB moiety folds back into the minor groove and stabilizes the DNA probe-target duplex. The effect of this stabilization is an increase in melting temperature [22]. Our home-made assay was then employed to evaluate and compare the miRNAs expression profiles in serum samples from PID, XLA, and healthy control subjects.

Material and Methods

Clinical Samples

A total of 12 pediatric patients were included and grouped according to the updated classification of PID introduced by the Expert Committee of International Union of Immunological Societies (IUIS) on PID [23]. All patients were seropositive for EBV infection. Nine EBV-seropositive patients affected by molecularly proven XLA, regularly followed up at the Pediatric Clinic, University of Turin, and 10 age- and sex-matched EBV-seropositive healthy controls were also enrolled in this study. Informed consent from all patients' parents was obtained. A total of 31 whole-blood samples were previously collected in red-top Vacutainer tubes (Becton–Dickinson, Rutherford, NJ, USA). Blood samples were left at room temperature for 30 min to allow complete coagulation. Coagulated samples were then spun at 1500 g for 15 min at 4 °C to separate serum. The serum was transferred to a new CryoTube (Nunc, Rochester, NY, USA). Serum samples were immediately frozen at −80 °C until RNA extraction.

Measurement of EBV DNA load was made while the patients remained in the hospital or when the physicians thought it necessary in the follow-up. Quantification of EBV DNA was carried out by a real-time quantitative PCR assay based on the TaqMan system.

Assay Design

Based on the stem loop technology described by Chen et al. [21], a method for miRNAs detection has been developed (Fig. 1).

Real-time primers and Taqman MGB probes were designed by Primer Express Software 3.0 (Life Technologies, Carlsbad, CA, USA) and recognizing miR-BART2-5p, miR-BART15 and miR-BART22 EBV miRNA sequences. SLP was designed in order to hybridize the first 6 nucleotides of 3′ end of the mature miR-BART2-5p, miR-BART15 and miR-BART22 miRNAs, while the stem-loop portion, constituted by 38 nucleotides, was considered for a universal reverse primer binding. Furthermore, forward primer was designed considering the first 12–17 nucleotides of cDNA, with the addition of 3–7 nucleotides at 5′ end to obtain a 60 °C Tm oligonucleotide. As half the miRNA length is covered by the forward primer, a MGB probe was found more suitable for the assay optimization. Secondary structure analysis of the amplicon was performed with ''mfold'' analysis (http://mfold.rna.albany.edu/?q=mfold/) to assure the complete distension of the amplicon during the annealing phase of enrichment step. A set of stem loop primers was also designed for miR-BART2-5p, miR-BART15 and miR-BART22 and small nucleolar RNA (snRNA) RNU43 detection. The sequences of all primer and probe sets are summarized in Table 1.

All Oligos were purchased from Life Technologies, (Carlsbad, CA, USA). To determine the specificity of each miRNA-specific primer, BLAST analysis was carried out using NCBI Nucleotide software (http://blast.ncbi.nlm.nih.gov/).

miRNA Isolation, cDNA Synthesis, and Real-Time PCR

400 µl of thawed serum or freshly isolated serum was purified by a novel protocol [24]. Briefly, 400 µL of serum was put into a 2-mL microcentrifuge tube with 1 mL of TRI reagent. Following vortexing and incubation, 1 µL of (1 µg/uL) nuclease-free glycogen was added to each tube and incubated at room temperature for 10 min. Then, 200 µL of chloroform was added to each tube and shaked vigorously for 20 s. Tubes should not be vortexed at this stage. Due to the time involved in each stage of processing, we recommend that a maximum of 12 tubes has to be processed at one time. The tubes were incubated at room temperature for 15 min and centrifuged at 12,000×*g* for

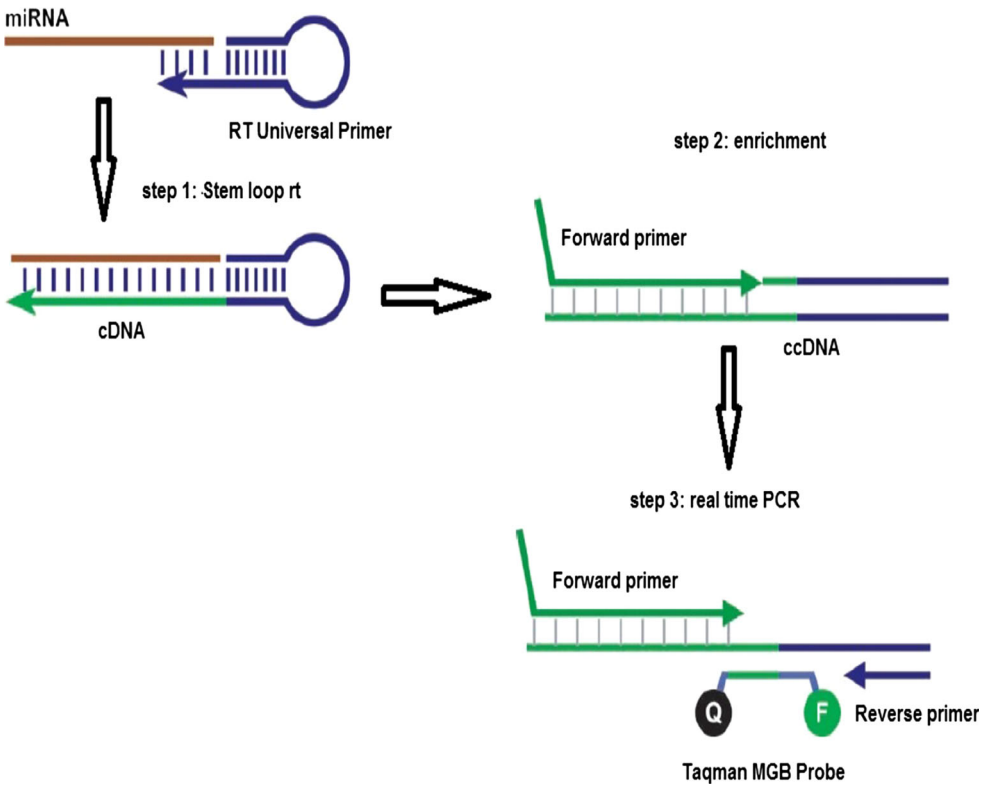

Fig. 1 Schematic representation of the principles of novel reverse transcription real-time PCR. The novel assay includes RT, enrichment step by asymmetric PCR, and real-time PCR. First, the Stem-loop RT primers bind the 3′ portion of miRNA molecules that are reverse transcribed by reverse transcriptase. Subsequently, the RT product is extended using an overlap PCR. Finally, the extended RT product is quantified using MGB TaqMan PCR

Table 1 Primers and probes list and miRNAs target sequences

Target	RNU43
Sequence	GAACUUAUUGACGGGCGGACAGAAACUGUGUGCUGAUUGUCAC GUUCUGAUU
SLP	GGCTCTGGTGCAGGGTCCGAGGTATTCGCACCAGAGCCAATCAG
Forward	TGACGGGCGGACAGAAA
Probe MGB fam	TGTGTGCTGATTGTCA
Target	MirBART2-5p
Sequence	UAUUUUCUGCAUUCGCCCUUGC
SLP	GGCTCTGGTGCAGGGTCCGAGGTATTCGCACCAGAGCCGCAAGG
Forward	CGCAGTATTTTCTGCATTCGC
Probe MGB fam	CCTTGCGGCTCTGG
Target	MirBART15
Sequence	GUCAGUGGUUUUGUUUCCUUGA
SLP	GGCTCTGGTGCAGGGTCCGAGGTATTCGCACCAGAGCCTCAAGG
Forward	CGCAGGTCAGTGGTTTTGTT
Probe MGB fam	TCCTTGAGGCTCTGG
Target	mirBART22
Sequence	UUACAAAGUCAUGGUCUAGUAGU
SLP	GGCTCTGGTGCAGGGTCCGAGGTATTCGCACCAGAGCCACTACT
Forward primer	CGCAGTTTTTTACAAAGTCATGG
Probe MGB fam	TCTAGTAGTGGCTCTGG
Universal reverse primer	TGCAGGGTCCGAGGTATTC

All sequences are in written in 5′-3′ direction

15 min at 4 °C. Then 800 µL of the upper aqueous phase was transferred to a 2-mL microcentrifuge tube and 1.2 mL of isopropanol was added to each tube. After 10-min incubation, the tubes were centrifuged at 12,000×*g* for 8 min at 4 °C and the supernatant was eliminated. Two 75 % ethanol lavages were performed and the tubes were allowed to dry out for 5 min at room temperature. 20 µL of nuclease-free water was added to each tube and the pellet was resuspended thoroughly. The RNA was always stored on ice after this stage. RNA purity and concentration were evaluated by spectrophotometry using NanoDrop ND-2000 (Thermo Fisher Scientific, Wilmington (DE) USA). 260/230 and 260/280 Absorbance ratios were used to assess the presence of contaminants: peptides, phenols, aromatic compounds, or carbohydrates and proteins. miRNAs reverse transcription (starting from 500 ng of total RNA) was carried out with Gene Amp RNA PCR kit (Life technologies, Carlsbad, CA, USA) including some modifications: 50 U of MMLV RT, 1 mM dNTPs, 5 mM $MgCl_2$, 1 U RNase Inhibitor, 1× PCR Buffer II and 0,5 µg of specific SLP (Table 1). The reaction was performed with an initial incubation at 16 °C for 30 min followed by a second step at 42 °C for 1 h. In order to end the reverse transcription step, a final incubation at 99 °C for 5 min was performed. After the reverse transcription step, an asymmetric PCR using 300 nM of specific forward primer (Table 1), 0,1 U of GoTaq® Hot Start polymerase (Promega, Bergamo, Italy), 4 µL of 5× Colorless GoTaq® Flexi Buffer and 2 µL of cDNA, obtaining a final volume of 20 µL, was carried out. The thermal profile used was 95 °C for 2 min; 30 cycles of 94 °C for 15 s, 55 °C for 30 s and 72 °C for 20 s. Five microliters of enriched cDNA, denominated ccDNA, was added to 35 µL of reaction mix containing 800 nM of forward primer, 1000 nM of Universal Reverse primer, 200 nM of MGB probe and 1× TaqMan Universal PCR Master Mix (P/N: 4324018 Life Technologies, Carlsbad, CA, USA) in a final volume of 40 µL. The amplifications were performed on ABI 7500 real-time PCR system (Life Technologies, Carlsbad, CA, USA) in a 96-well plate at 95 °C for 10 min, followed by 40 cycles of 95 °C for 15 s and 60 °C for 1 min. Each sample was run in technical triplicate.

The level of miRNAs expression was measured using the Cq (cycle quantification) value, the fractional cycle number at which the fluorescence of each sample passed a fixed threshold. During PCR, changing reaction conditions and environment can influence fluorescence. In general, the level of fluorescence in any one well corresponds to the amount of target present. Fluorescence levels may fluctuate due to changes in the reaction medium creating a

background signal. The background signal is most evident during the initial cycles of PCR prior to significant accumulation of the target amplicon. During these early PCR cycles, the background signal in all wells is used to determine the "baseline fluorescence" across the entire reaction plate. The goal of data analysis is to determine when target amplification is sufficiently above the background signal, facilitating more accurate measurement of fluorescence. The threshold is the numerical value assigned for each run, which reflects a statistically significant point above the calculated baseline.

The $2^{-\Delta\Delta Cq}$ method for relative quantification of gene expression was used to determine the level of miRNA expression. ΔCq was calculated by subtracting the Cq value of RNU43 RNA from the Cq value of the miRNA of interest. The fold change was calculated using the equation Fold change $= 2^{-\Delta\Delta Cq}$.

Real-Time RT-PCR Performance Analysis

Dynamic range, sensitivity, specificity, intra- and inter-assay variation, R^2 value, slope and efficiency were analyzed in order to define the test performance.

Dynamic range was evaluated considering serial logarithmic scale dilutions of specific purified amplicons for each miRNA analyzed. Serial dilution was executed from a stock of 10^9 copies/reaction solution, obtained after a quantification based on the A260 value, and 8 serial dilutions (from 10^8 to 10^0) for a specific miRNA were produced.

Sensitivity was defined through the lower dilution detected by the test in 100 % of cases. The detection ability was estimated by four replicates of each dilution (100 copies, 10 copies, and 1 copies/reaction) (Table 2).

Specificity was tested by the specific amplification and detection of each EBV miRNA in a pool containing amplicons of the three EBV miRNAs (miR-BART2-5p, miR-BART15, and miR-BART22) and two human miRNAs (hsa-miR-155 and hsa-miR-146a), respectively, in a 10^3 copies/reaction concentration.

Table 2 Sensitivity test with three different concentrations (100, 10, 1 copy/reaction)

MiRNA name	100 copies	10 copies	1 copy
MirBART2-5p	4/4	2/4	2/4
MirBART15	4/4	2/4	2/4
mirBART22	4/4	2/4	2/4

The fraction expresses the positive detection on the number of tests performed

Intra- and inter-assay variations were evaluated by three replicates at four different concentrations (10^2 to 10^6 copies/reaction) in each run and repeated in 3 consecutive days. The variation observed was expressed as coefficient of variation (CV) (Table 3).

Slope and R^2 value were obtained from the ABI 7500 real-time PCR system (Life Technologies, Carlsbad, CA, USA) instrument, as expression respectively of the amplification curve and of the goodness-of-fit of linear regression.

Efficiency was estimated using the formula efficiency $= 10^{(-1/\text{slope})} - 1$.

Statistical Analysis

Kruskal–Wallis one-way analysis of variance test (ANOVA) was used in order to establish statistical significant differences of miRNA levels among the three populations (PID, XLA, Healthy patients) tested. A P value < 0.05 was considered statistical significant.

Results

In this study, a new real-time RT–PCR approach was proposed for miRNA quantification, outlined in Fig. 1. It included three steps: RT, enrichment/pre-PCR and real-time PCR. First, the stem–loop RT primer hybridizes to a target miRNA molecule which is subsequently reverse transcribed by a Multi-Scribe reverse transcriptase. The RT products are then enriched using an asymmetric PCR and amplified through real-time MGB TaqMan PCR.

Specific stem-loop primers, specific forward primers, universal reverse primer, and TaqMan probe are listed in Table 1. The confirmation that primers and probes sequences did not recognize other known sequences was obtained by NCBI Nucleotide BLAST software analysis. The assay specificity observed was 100 % and showed excellent linearity with a dynamic range of at least 7 logs, able to detect as few as 100 copies in the PCR reaction (Fig. 2).

The sensitivity, defined as the lowest amount of target DNA detected by the assay, was defined as the concentration where the assay was positive in all four replicates and was attested to 100 copies/reaction for all of the three miRNAs. Intra- and inter-assay variations for the Cq values showed CVs, respectively, lower than 0.88 and 1.65 % for miBART2-5p, 2.42 and 2.14 % for miBART15, and 0.76 and 1.46 % for miBART22 (Table 3). Furthermore, R^2 values, or the coefficient of correlation, were repeatedly higher than 0.996 and the slopes of the standard curves greater than −3.39, indicating consistently high

Table 3 Intra-assay and Inter-assay variation of miR-BART2-5p, miR-BART15, and miR-BART22

	Intra-assay Cq values			Inter-assay Cq values		
	Mean	SD	CV (%)	Mean	SD	CV (%)
miR-BART2-5 copies/reaction						
100	31.12667	0.274651	0.882367	31.09333	0.253837	0.816372
1000	28.15	0.1253	0.445114	28.25	0.20664	0.731468
10,000	24.58333	0.152753	0.621366	24.38333	0.404145	1.657465
100,000	21.02333	0.115902	0.551303	21.03333	0.126623	0.60201
1,000,000	17.82667	0.061101	0.342751	17.94333	0.145717	0.812093
miR-BART15 copies/reaction						
100	35.66	0.866083	2.428724	35.99333	0.770346	2.140247
1000	33.20667	0.538733	1.622364	33.54	0.637887	1.90187
10,000	29.95667	0.257747	0.860398	30.02333	0.355575	1.184328
100,000	27.29	0.1249	0.457677	27.22333	0.094516	0.347189
1,000,000	23.94667	0.047258	0.197348	23.94333	0.051316	0.214323
miR-BART22 copies/reaction						
100	32.12	0.108167	0.336758	32.45333	0.474377	1.46172
1000	29.89333	0.208167	0.696365	30.22667	0.378594	1.252516
10,000	26.6	0.060828	0.228675	26.7	0.20664	0.773932
100,000	23.11	0.14	0.605798	23.07667	0.113725	0.492813
1,000,000	19.48333	0.148436	0.761863	19.41667	0.167432	0.862309

Intra-assay and inter-assay variations obtained from mir-BART2-5p, miR-BART15, and miR-BART22 scalar dilutions ranging from 10^2 to 10^6 copies/reaction

SD standard deviation, *CV (%)* coefficient of variation expressed as percentage

amplification efficiency (higher than 97 %). All the data depicting standard deviations and coefficient of variations for each standard concentration are shown in Table 3.

The assay was then optimized and validated through biological samples testing. miR-BART2-5p, miR-BART15, and miR-BART22 were quantified by real-time RT-PCR in serum samples of 3 study groups: 12 patients with PID, 9 patients with XLA and 10 healthy controls. After measuring the expression of the snRNA RNU43 as a housekeeping miRNA, the miRNA data were normalized by calculating the relative $2^{-\Delta\Delta Cq}$ value. Preliminary experiments were performed using the plasma samples, and snRNA RNU43 was considered to be appropriate as an endogenous control (data not shown). The miR-BART22 plasma levels in patients with PID were significantly higher than those in patients with XLA and in controls ($P = 0.0001$) (Fig. 3). On the contrary, miR-BART2-5p and miR-BART15 plasma levels did not exhibit significant differences in term of expression levels compared to the PID, XLA and healthy controls group (Fig. 3).

After the validation of the assay, we compared the miRNA results with EBV viral load. No correlation was demonstrated with Pearson test, $r^2 = 0.2047$; 0.047 and 0.040 for miR-BART15, miR-BART2-5 and miR-BART22, respectively (Fig. 4; Table 4).

Discussion

Currently, miRNAs are opening their way for their routine implementation in clinical diagnosis and prognosis of a diverse range of diseases. However, increasing acceptance and utilization of molecular-based miRNA assays for research and diagnostic purposes necessitate the existence of a rigorous validation before their use in clinical diagnosis. Microarray is the most widely used high-throughput technique for the identification of a cancer-specific miRNA expression profile, but the low level of sensitivity is a disadvantage of this technique as it is difficult to amplify miRNA targets and can lead to false positive signals from closely related miRNAs and genomic sequences [25]. RT-qPCR, on the contrary, is a powerful technique for quantifying gene expression in the life sciences and medicine as it is highly sensitive, accurate, and simple [26]. Moreover, it is the most adaptive technique for the quantification of miRNAs used by the general research community. Several RT-qPCR assays have been established for miRNA quantification, and are currently made available by companies. Considering the similar small size of miRNAs with ordinary PCR primers, we proposed an optimal and convenient alternative process based on readily available techniques and materials.

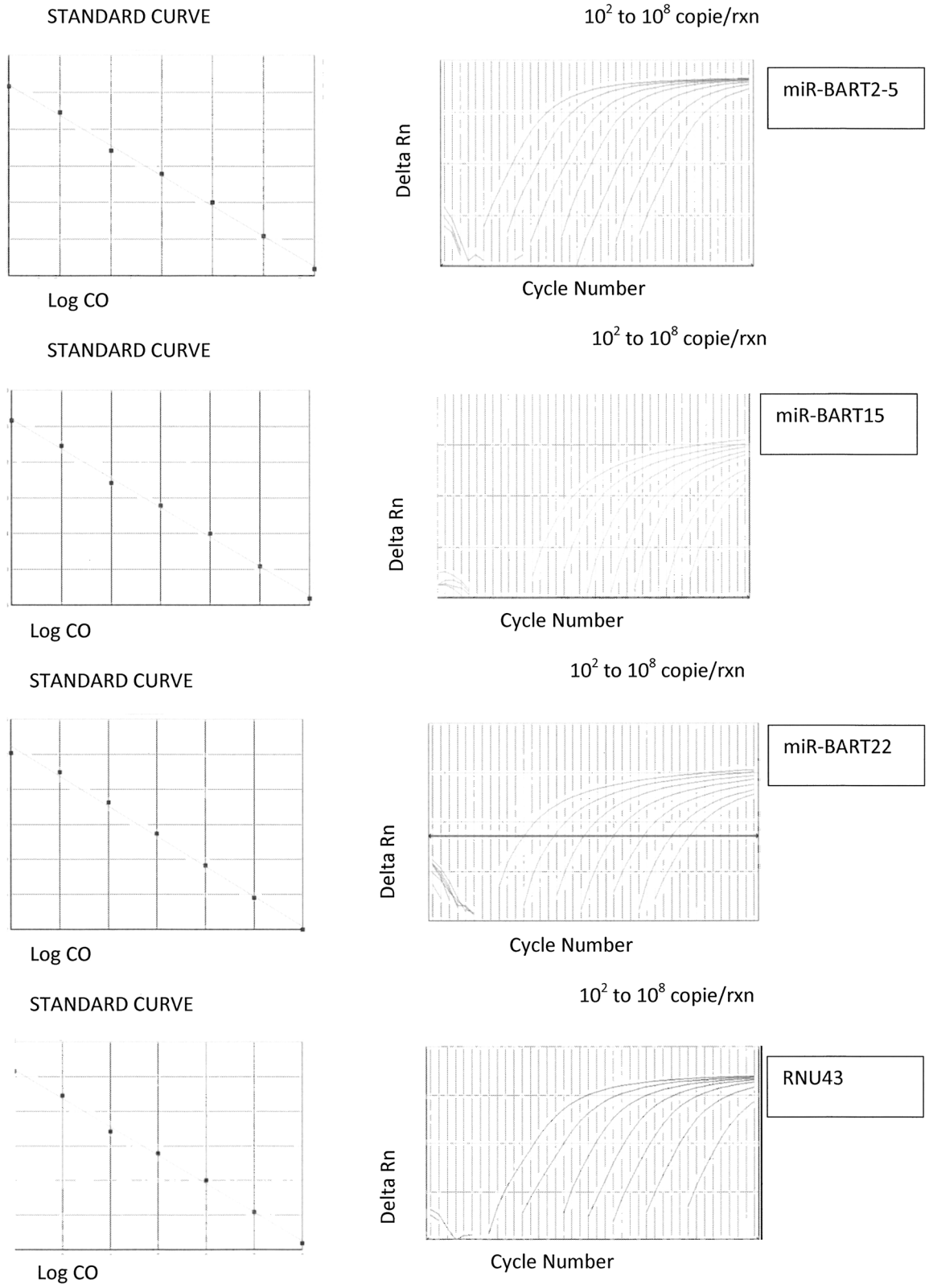

Fig. 2 Dynamic range of the stem–loop RT real-time PCR assay. Amplification curve was obtained with sevenfold serial dilutions of miR-BART2-5p, miR-BART15, miR-BART22, and RNU43 cDNA ranging from 10^8 to 10 copies/rxn. The number of PCR cycles is expressed on x-axis and normalized fluorescence intensity (Delta Rn) on y-axis

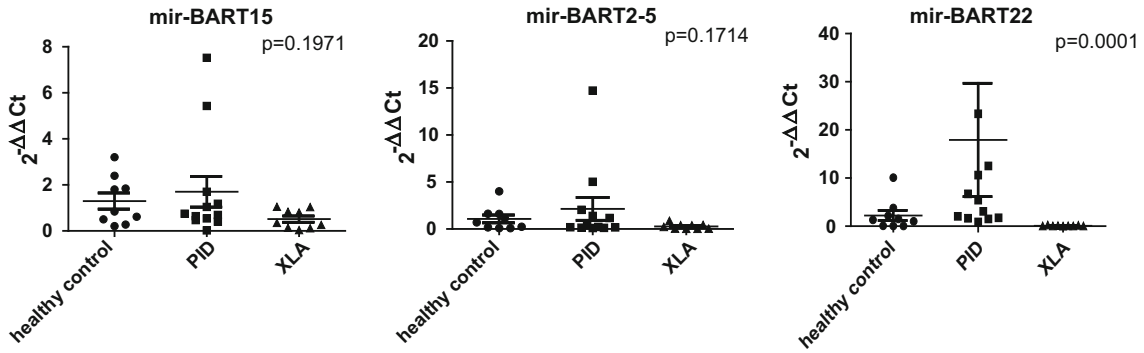

Fig. 3 XLA miR-BART15, miR-BART2-5p, and miR-BART22 expression levels in healthy control, PID (primary immunodeficiency) and XLA (type of BTK mutations) patients. Statistical analysis was performed by Anova test Kruskal–Wallis. *p* *P*-value

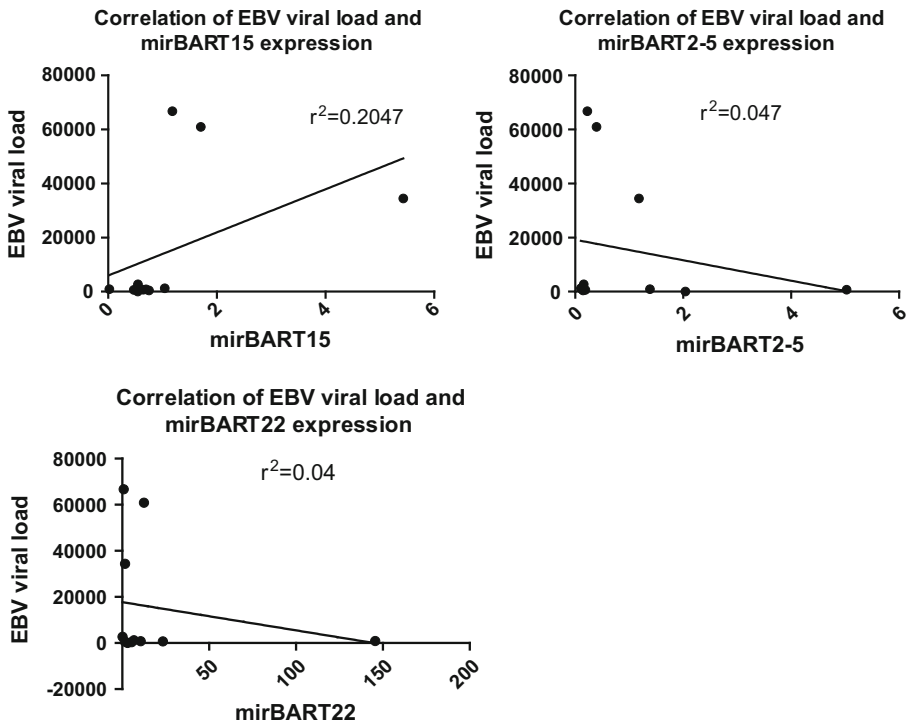

Fig. 4 Correlations were calculated for all miRNAs analyzed by qPCR and for all individuals. The three correlations by the Pearson method are shown, along with the coefficient of determination. The x-axis units are delta–delta Ct (normalized, then related to the mean expression of control samples), which represents relative abundance. The y-axis units are value of viral load expressed in copies/ml of blood

The most important consideration for this assay design was to know the precise sequence of the miRNA of interest. Deep sequencing results have shown both 5′ and 3′ variations in newly discovered miRNAs and shortened 5′ and/or 3′ ends may arise from degradation during processing of the sample. However, it is probable that the sequence represented in greatest abundance could be the entire one. The forward real-time PCR primer and Probe were designed to obtain a maximal and simultaneous cover of the mature miRNA sequence. In order to achieve this goal, the probe length should be between 12 and 17 nucleotides, with an ideal Tm close to 70 °C. For this reason, the choice was to use an MGB probe that raised probe's Tm and confers higher specificity.

Recently, the role of miR-BART2-5p, miR-BART15, and miR-BART22 has been evaluated in diseases such as CAEBV, PTLD, and cancer [27]. miR-BART2-5p down-regulates the viral DNA polymerase BALF5, thereby inhibiting the transition from latent to lytic viral replication and thus maintaining EBV latency so as to prevent host immune attack [28]. miR-BART2-5p also protects EBV-infected cells from recognition and killing by NK cells, targeting the major histocompatibility complex class I-related chain B gene [29]. miR-BART15 has been reported to suppress the production of the p53-upregulated modulator of apoptosis [30]. Inhibition of this protein protects cells from apoptosis, indicating that this EBV miRNA might be important in promoting tumor cell survival. miR-BART22

Table 4 $2^{-\Delta\Delta Cq}$ value of mirBART22, mirBART2-5, and mirBART15 and corresponding EBV viral load

Sample PID	$2-^{\Delta\Delta Cq}$ mirBart22	$2-^{\Delta\Delta Cq}$ mirBart2-5	$2-^{\Delta\Delta Cq}$ mirBart15	EBV viral load copies/ml blood
1	0.88	0.22	1.18	66,700
2	23.36	5.02	0.64	700
3	145.61	1.38	0.02	900
4	6.70	0.10	1.04	1200
5	3.08	2.04	0.54	0
6	1.74	0.17	0.40	nd
7	5.41	0.14	0.75	400
8	0.14	0.15	0.54	2700
9	1.52	0.18	0.47	600
10	10.60	0.12	0.69	800
11	12.51	0.39	1.70	60,900
12	1.64	1.18	5.43	34,400

causes a reduction of the levels of LMP2, a highly immunogenic protein. Expression of this miRNA protects EBV-infected cells from the host immune response [31]. These miRNAs may contribute to persistent virus infection. In PID subject, the persistence of EBV infection may lead to lymphoproliferative disorders. The existence of a growing body of evidence concerning the value of miR-BART2-5p, miR-BART15, and miR-BART22 expression pattern in many of the mentioned diseases requires the existence of a validated and cost-effective home-brew assay for its reliable quantification.

Collectively, considering the lack of in vitro diagnostics assays and the need to have a reliable quantitative assay for miR-BART2-5p, miR-BART15, and miR-BART22, we have developed a new assay for detection and quantification of these miRNAs. This new approach showed an enhanced dynamic range of seven orders of magnitude and the general detection limit of about 71 zg (zeptograms) miRNA. These data establish that the new real-time RT-PCR approach could be particularly useful for the quantification of low copy number or under-expressed miRNAs thanks to the optimal efficiency achieved in the range of 7.1 pg—7.1 ag (attograms) of total RNA. Moreover, stem-loop RT primer was used instead of linear adaptor to make sure that this protocol is insensitive to double-stranded nucleic acid molecules, as the spatial constraint of the stem-loop structure might prevent the RT primer from binding double-stranded genomic DNA molecules and enhance the thermal stability of the RNA-DNA heteroduplex [21].

The assay developed in the present study showed a maximum CV value of 2.42 and 2.14 % for intra-assay and inter-assay, respectively, and a reproducible quantification of miR-BART2-5p, miR-BART15, and miR-BART22 within the dynamic range of 10^8–10^2 copies/reaction, as previously reported by Amoroso et al. [32]. The dynamic range of the assay encompassed 7 orders of magnitude (with miR-BART2-5p, miR-BART15, and miR-BART22 R^2 values respectively of 0.999, 0.9977, 0.9961) (Fig. 2). Analytical sensitivity of 100 % was achieved with 10^2 copies/reaction of miR-BART2-5p, miR-BART15, and miR-BART22 cDNA. Similar assays to ours were previously developed [27, 32], using specific miRNA kit for the retro transcription. Furthermore, the novelty of this work consisted in the addition of an enrichment step by asymmetric PCR, after a conventional retrotranscription, to obtain a more efficient real-time amplification. Undoubtedly, the quality of RNA extraction may affect miRNA amplification, and, therefore, optimizing extraction protocol for each sample type can provide acceptable amplification consistency. So, a modified RNAzol extraction protocol as proposed by Taylor and colleagues [24] was used. RNU43 was employed as housekeeping gene for its similar length to miRNAs as well as feasibility of applying the same designing strategy as miRNAs for its detection. This reliable home-brew assay and its use as an open source tool could provide an external evaluation by other researchers. The use of modified RNAzol protocol for total RNA extraction instead mirVana^{TM} miRNA Isolation Kit (Thermo Fisher Scientific Carlsbad, CA, USA) could provide the chance of improvement and the costs decrease of test performance. The RNA extraction method with mirVana kit is tenfold more expensive than RNAzol modified protocol. The cost advantage is even more evident when screening very large sets of hundreds or thousands of samples. This assay might be used to determine minimum and maximum normal thresholds of miR-BART2-5p, miR-BART15, and miR-BART22 expressions in different forms

of disease states, which could assist the clinicians for better prognosis assessment and therapy, as suggested by Kawano et al. [27] who considered plasma miR-BART2-5p and miR-BART15 levels potentially biomarkers for achieving complete remission to EBV infections.

Furthermore, EBV-encoded miR-BART7 levels have also been suggested to be useful for diagnostic screening [33]. EBV miRNAs are differentially expressed in lymphoid cells and under three different virus latency programs, distinguished from each other by the pattern of EBV antigens produced in EBV-positive cells. EBV-encoded nuclear antigen 1 (EBNA1) is produced in latency type I, only, as in Burkitt lymphoma; while latent membrane protein 1 (LMP1) and LMP2, as well as EBNA1, are produced in latency type II, as in Hodgkin disease, nasopharyngeal carcinoma, and CAEBV infection. Highly immunogenic EBNA3 proteins are produced together with other EBV-latent antigens, in latency type III, as in IM (Infectious Mononucleosis) [34]. The BHRF1 miRNAs are exclusively expressed at high levels in cells displaying type III EBV latency [35], and these miRNAs are not detected in infections with latency types I and II [13, 36]. On the other hand, Pratt et al. [37]. demonstrated that the expression levels of BART miRNAs were greater in nasopharyngeal carcinoma and gastric carcinoma cell lines (both of which exhibit latency type II), compared with levels in other cell lines with latency I or III. Kawano et al. [27] recently speculated that the plasma viral load at diagnosis is an indicator of the amount of EBV-infected cells infiltrating organs, such as the liver and spleen. On the basis of this speculation, plasma samples may have an advantage for evaluating disease status in CAEBV infection for endogenous virus-associated miRNAs. In this study, increased expression levels of miR-BART22 in PID samples compared to XLA and healthy patients (Fig. 3) were observed. Considering that miR-BART22 causes a reduction of the levels of LMP2, a highly immunogenic protein, this high miRNA expression could protect EBV-infected cells from the host immune response [31] and contribute to persistent virus infection [26]. The expression levels of miR-BART2-5p and miR-BART15, on the contrary, did not differ from PID, XLA, and healthy subjects (Fig. 3). LCLs can only be taken as a model for some of the lymphomas that develop in patients with an immunodeficiency. However, there are many types of EBV-associated cancers in which the EBV miRNAs are expressed. The identification of the mRNAs that mediate the functions ascribed to the EBV miRNAs proved to be more difficult. High-throughput and bioinformatics methods have identified several hundreds of genes, validated interaction between mRNAs and the viral miRNAs for a few of them but it remains difficult to demonstrate that a given protein mediates the functions ascribed to the miRNAs. The spatiotemporal expression patterns of miRNAs are important for the verification of their predicted function. There is an urgent need for a highly specific and simple method for quantification of miRNA. This study reports the correlation of miRNA profiles in PID versus EBV viral load. Although we demonstrated no correlation, this represents an important step in the knowledge of the role of miRNA in immunodeficiency patients. Recent data demonstrate that BART miRNAs expression is also significantly induced during lytic replication of EBV [38] in the presence of high viral load; however, expression of the BART miRNAs cluster is also characteristic of latent EBV infection [39]. Opposite to our findings, Gao et al., demonstrated a positive correlation between viral loads and some EBV-miRNAs (miR-BHRF1-2-3p, miR-BHRF1-2-5p, miR-BHRF 1–3, miR-BART2-5p, miR-BART3-5p, miR-BART5-5p, miR-BART17-3p, miR-BART6-3p, miR-BART6-5p, miR-BART21-5p, miR-BART7-3p, miR-BART7-5p, miR-BART8-5p, miR-BART12-1, miR-BART19-3p, miR-BART20-5p, miR-BART13*-1, and miR-BART14*-1). Cameron et al. [40] showed that most of the BART miRNAs are essential for B cell transformation. Mature EBV-miRNAs are secreted by EBV-infected B cells through exosomes, and exosomes can protect EBV-miRNAs from degradation by RNases. This could explain why some patients with higher EBV-miRNAs did not have measurable EBV DNA loads in plasma or *viceversa*. From a practical point of view our method offers an alternative for scientists to quantify multiple miRNA expression in the same sample and we are currently improving the assay to reach the possibility to detect a wider pattern of EBV miRNAs.

Acknowledgments The authors thank the colleagues of the Department of Public Health and Pediatrics. The study was sponsored by Fondazione Giovanni Goria.

References

1. Ghildiyal, M., & Zamore, P. D. (2009). Small silencing RNAs: an expanding universe. *Nature Reviews Genetics, 10*, 94–108.
2. Baltimore, D., Boldin, M. P., O'Connell, R. M., Rao, D. S., & Taganov, K. D. (2008). MicroRNAs: new regulators of immune cell development and function. *Nature Immunology, 9*, 839–845.
3. Ivey, K. N., & Srivastava, D. (2010). MicroRNAs as regulators of differentiation and cell fate decisions. *Cell Stem Cell, 7*, 36–41.
4. Tili, E., Michaille, J. J., Costinean, S., & Croce, C. M. (2008). MicroRNAs, the immune system and rheumatic disease. *Nature Clinical Practice Rheumatology, 4*, 534–541.
5. Di Leva, G., & Croce, C. M. (2010). Roles of small RNAs in tumor formation. *Trends in Molecular Medicine, 16*, 257–267.
6. Du, L., & Pertsemlidis, A. (2011). Cancer and neurodegenerative disorders: pathogenic convergence through microRNA regulation. *Journal of Molecular Cell Biology, 3*, 176–180.
7. Kincaid, R. P., & Sullivan, C. S. (2012). Virus-encoded microRNAs: an overview and a look to the future. *PLoS Pathogens, 8*(12), e1003018.

8. Umbach, J. L., Nagel, M. A., Cohrs, R. J., Gilden, D. H., & Cullen, B. R. (2009). Analysis of human alpha herpesvirus microRNA expression in latently infected human trigeminal ganglia. *Journal of Virology, 83*, 10677–10683.
9. Harwig, A., Das, A. T., & Berkhout, B. (2015). HIV-1 RNAs: sense and antisense, large mRNAs and small siRNAs and miRNAs. *Current Opinion in HIV and AIDS, 10*, 103–109.
10. Umbach, J. L., Kramer, M. F., Jurak, I., Karnowski, H. W., Coen, D. M., & Cullen, B. R. (2008). MicroRNAs expressed by Herpes simplex virus 1 during latent infection regulate viral mRNAs. *Nature, 454*, 780–783.
11. Bellare, P., & Ganem, D. (2009). Regulation of KSHV lytic switch protein expression by a virus-encoded microRNA: an evolutionary adaptation that fine-tunes lytic reactivation. *Cell Host & Microbe, 6*, 570–575.
12. Lei, X., Bai, Z., Ye, F., et al. (2010). Regulation of NF-κB inhibitor IκBα and viral replication by a KSHV microRNA. *Nature Cell Biology, 12*, 193–199.
13. Klinke, O., Feederle, R., & Delecluse, H. J. (2014). Genetics of Epstein-Barr virus microRNAs. *Seminars in Cancer Biology, 26*, 52–59.
14. Ferracin, M., Veronese, A., & Negrini, M. (2010). Micromarkers: miRNAs in cancer diagnosis and prognosis. *Expert Review of Molecular Diagnostics, 10*, 297–308.
15. Pfeffer, S., Zavolan, M., Grässer, F. A., Chien, M., Russo, J. J., Ju, J., et al. (2004). Identification of virus-encoded microRNAs. *Science, 304*, 734–736.
16. Gao, L., Ai, J., Xie, Z., Zhou, C., Liu, C., Zhang, H., & Shen, K. (2015). Dynamic expression of viral and cellular microRNAs in infectious mononucleosis caused by primary Epstein-Barr virus infection in children. *Virology Journal, 12*, 208. doi:10.1186/s12985-015-0441-y.
17. Brase, J. C., Wuttig, D., Kuner, R., & Sultmann, H. (2010). Serum microRNAs as noninvasive biomarkers for cancer. *Molecular Cancer, 9*, 306–310.
18. Moussay, E., Wang, K., Cho, J. H., et al. (2011). MicroRNA as biomarkers and regulators in B-cell chronic lymphocytic leukemia. *Proceedings of the National Academy of Sciences of the United States of America, 108*, 6573–6578.
19. Lim, L. P., Glasner, M. E., Yekta, S., Burge, C. B., & Bartel, D. P. (2003). Vertebrate microRNA genes. *Science, 299*, 1540–1545.
20. Liang, R. Q., Li, W., Li, Y., et al. (2005). An oligonucleotide microarray for microRNA expression analysis based on labeling RNA with quantum dot and nanogold probe. *Nucleic Acids Research, 33*, e17.
21. Chen, C., Ridzon, D. A., Broomer, A. J., et al. (2005). Real-time quantification of microRNAs by stem-loop RT-PCR. *Nucleic Acids Research, 33*, e179.
22. Yao, Y., Nellåker, C., & Karlsson, H. (2006). Evaluation of minor groove binding probe and Taqman probe PCR assays: Influence of mismatches and template complexity on quantification. *Molecular and Cellular Probes, 20*, 311–316.
23. Geha, R. S., Notarangelo, L. D., Casanova, J. L., et al. (2007). Primary immunodeficiency diseases: an update from the international union of immunological societies primary immunodeficiency diseases classification committee. *Journal of Allergy and Clinical Immunology, 120*, 776–794.
24. Bergallo, M., Gambarino, S., Martino, S., et al. (2015). Comparison of two available RNA extraction protocols for microRNA amplification in serum samples. *Journal of Clinical Laboratory Analysis*. doi:10.1002/jcla.21848.
25. Huang, P. C., Chen, C. Y., Yang, F. Y., & Au, L. C. (2009). A multisampling reporter system for monitoring microRNA activity in the same population of cells. *BioMed Research International, 10*, 471–476.
26. Giulietti, A., Overbergh, L., Valckx, D., et al. (2001). An overview of real-time quantitative PCR: Applications to quantify cytokine gene expression. *Methods, 25*, 386–401.
27. Kawano, Y., Iwata, S., Kawada, J., et al. (2013). Plasma viral microRNA profiles reveal potential biomarkers for chronic active Epstein-Barr virus infection. *Journal of Infectious Diseases, 208*, 771–779.
28. Barth, S., Pfuhl, T., Mamiani, A., et al. (2008). Epstein-Barr virus-encoded micro- RNA miR-BART2 down-regulates the viral DNA polymerase BALF5. *Nucleic Acids Research, 36*, 666–675.
29. Nachmani, D., Stern-Ginossar, N., Sarid, R., & Mandelboim, O. (2009). Diverse herpesvirus microRNAs target the stress-induced immune ligand MICB to escape recognition by natural killer cells. *Cell Host & Microbe, 5*, 376–385.
30. Choy, E. Y., Siu, K. L., Kok, K. H., et al. (2008). An Epstein-Barr virus-encoded micro- RNA targets PUMA to promote host cell survival. *Journal of Experimental Medicine, 205*, 2551–2560.
31. Lung, R. W., Tong, J. H., Sung, Y. M., et al. (2009). Modulation of LMP2A expression by a newly identified Epstein-Barr virus-encoded microRNA miR-BART22. *Neoplasia, 11*, 1174–1184.
32. Amoroso, R., Fitzsimmons, L., Thomas, W. A., Kelly, G. L., Rowe, M., & Bell, A. I. (2011). Quantitative studies of Epstein-Barr virus-encoded microRNAs provide novel insights into their regulation. *Journal of Virology, 85*, 996–1010. doi:10.1128/JVI.01528-10.
33. Chan, J. Y., Gao, W., Ho, W. K., Wei, W. I., & Wong, T. S. (2012). Overexpression of Epstein-Barr virus-encoded microRNA-BART7 in undifferentiated nasopharyngeal carcinoma. *Anticancer Research, 32*, 3201–3210.
34. Cohen, J. I. (2000). Epstein-Barr virus infection. *New England Journal of Medicine, 343*, 481–492.
35. Xia, T., O'Hara, A., Araujo, I., et al. (2008). EBV microRNAs in primary lymphomas and targeting of CXCL-11 by ebv-miR-BHRF1–3. *Cancer Research, 68*, 1436–1442.
36. Xing, L., & Kieff, E. (2007). Epstein-Barr virus BHRF1 micro- and stable RNAs during latency III and after induction of replication. *Journal of Virology, 81*, 9967–9975.
37. Pratt, Z. L., Kuzembayeva, M., Sengupta, S., & Sugden, B. (2009). The microRNAs of Epstein-Barr virus are expressed at dramatically differing levels among cell lines. *Virology, 386*, 387–397.
38. Yuan, J., Cahir-McFarland, E., Zhao, B., & Kieff, E. (2006). Virus and cell RNAs expressed during Epstein-Barr virus replication. *Journal of Virology, 80*, 2548–2565.
39. Cai, X., Schafer, A., Lu, S., Bilello, J. P., Desrosiers, R. C., Edwards, R., et al. (2006). Epstein-Barr virus microRNAs are evolutionarily conserved and differentially expressed. *PLoS Pathog, 2*, e23. doi:10.1371/journal.ppat.0020023.
40. Cameron, J. E., Fewell, C., Yin, Q., McBride, J., Wang, X., Lin, Z., et al. (2008). Epstein-Barr virus growth/latency III program alters cellular microRNA expression. *Virology, 382*, 257–266. doi:10.1016/j.virol.2008.09.018.